Heterogeneous & Homogeneous & Bio- & Nano-
CHEMCATCHEM
CATALYSIS

Accepted Article

Title: Enzymatic production of non-natural nucleoside-5'-monophosphates by a novel thermostable uracil phosphoribosyltransferase

Authors: Jon Del Arco, Javier Acosta, Humberto M. Pereira, Almudena Perona, Neratur K. Lokanath, Naoki Kunishima, and Jesús Fernández-Lucas

To be cited as: *ChemCatChem* 10.1002/cctc.201701223

Link to VoR: http://dx.doi.org/10.1002/cctc.201701223

A Journal of
ChemPubSoc Europe

WILEY-VCH www.chemcatchem.org

WILEY-VCH
10.1002/cctc.201701223

FULL PAPER

WILEY-VCH

Enzymatic production of non-natural nucleoside-5'-monophosphates by a novel thermostable uracil phosphoribosyltransferase

Jon del Arco,[a] Javier Acosta,[a] Humberto M. Pereira,[b] Almudena Perona,[a] Neratur K. Lokanath,[c] Naoki Kunishima, *[d] Jesús Fernández-Lucas *[a, e].

Abstract: The use of enzymes as biocatalysts applied to synthesis of modified nucleoside-5'-monophosphates (NMPs) is an interesting alternative to traditional multistep chemical methods which offers several advantages, such as stereo, regio and enantioselectivity, simple downstream processing, and mild reaction conditions. Herein we report the recombinant expression, production and purification of uracil phosphoribosyltransferase from *Thermus themophilus* HB8 (*Tt*UPRT). The structure of *Tt*UPRT has been determined by protein crystallography, and its substrate specificity and biochemical characteristics have been analysed, providing new structural insights into the substrate-binding mode. Biochemical characterization of the recombinant protein indicates that the enzyme is a homotetramer, with activity and stability across a broad range of temperatures (50-80 °C), pH (5.5-9) and ionic strength (0-500 mM NaCl). Surprisingly, *Tt*UPRT is able to recognize several 5 and 6-substituted pyrimidines as substrates. These experimental results, suggest *Tt*UPRT could be a valuable biocatalyst for the synthesis of modified NMPs.

Introduction

Nucleosides are essential metabolites in numerous biochemical processes. In this sense, nucleoside analogues have been widely used in the treatment of several serious human illnesses such as cancer or viral diseases, among others.[1-3].

The intracellular phosphorylation of nucleosides leads to corresponding nucleotides. In this regard, the availability of synthetic nucleotide analogues allows the study of structure-activity relationships, kinetics, and other metabolic consequences of nucleoside administration. As a consequence, the development of suitable and efficient methodologies for the synthesis of nucleoside-5'-mono- (NMPs), -di (NDPs) and triphosphates (NTPs) has been the target of several chemical and enzymatic synthetic efforts.[4-5] Moreover, 2'-deoxynucleoside-5'-monophosphates (dNMPs) are basic precursors of corresponding 2'-deoxynucleoside-5'-triphosphates (dNTPs), which are widely used in modern molecular biology experiments. In this respect, the development of new synthetic processes of NMPs and dNMPs is a main focus area of pharmaceutical companies.

Chemical synthesis of NMPs is commonly performed by 5'-phosphorylation of the precursor nucleosides. It often requires the use of chemical reagents (phosphoryl chloride, $POCl_3$, or phosphorus pentoxide, P_2O_5), acidic conditions and organic solvents which are expensive and environmentally harmful. [6] Indeed, chemical glycosylation of precursor nucleosides often requires time-consuming multistep processes.[7] These synthetic routes usually provide poor or moderate global yields and low product purity, and are also associated with harsh reaction conditions and waste disposal issues.

In this context, the enzymatic synthesis of NMPs shows many advantages, such as one-pot reactions under mild conditions, high stereo- and regio-selectivity, and an environmentally-friendly technology. Due to this, many different enzymes have been employed as valuable catalysts for mono or multi-enzymatic synthesis of NMPs,[8-12] including nucleoside kinases (NK),[13-15] acid phosphotransferases (AP/PTase),[16-17] 5'-phosphodiesterases[18] or phosphoribosyltransferases (PRT).[11-12, 19]

Uracil phosphoribosyltransferase (EC 2.4.2.9, UPRT) catalyzes the reversible transfer of the 5-phosphoribosyl group from 5-phospho-α-D-ribosyl-1-pyrophosphate (PRPP) to uracil N1 to form uridine-5'-monophosphate, UMP, in the presence of Mg^{2+} (Scheme 1).[20-22] Since UMP is a common precursor of all pyrimidine nucleotides, UPRT is an essential enzyme in the salvage pathways for pyrimidine nucleotide synthesis.

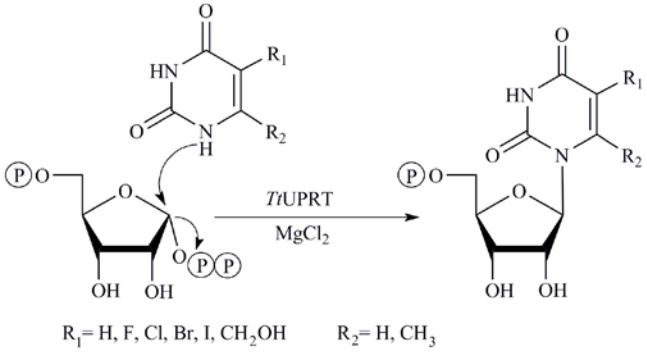

Scheme 1. Enzymatic synthesis of different pyrimidine nucleoside-5'-monophosphates catalyzed by *Tt*UPRT.

[a] J. del Arco, J. Acosta, Dr. A. Perona and Dr. J. Fernández- Lucas
Applied Biotechnology Group,
Universidad Europea de Madrid,
Urbanización El Bosque, Calle Tajo, s/n, 28670 Villaviciosa de Odón (Madrid), Spain.
E-mail: jesus.fernandez2@universidadeuropea.es
[b] Dr. HM Pereira
Instituto de Física de São Carlos, Universidade de São Paulo, CP369, 13560-970, São Carlos, SP, Brazil.
[c] Dr. Neratur K. Lokanath
Department of Studies in Physics, University of Mysore, Mysore 570 006, India
[d] Dr. Naoki Kunishima
RIKEN SPring-8 Center, 1-1-1 Kouto, Sayo, Hyogo 679-5148, Japan. E-mail: kunisima@spring8.or.jp
[e] Dr. J. Fernández- Lucas
Grupo de Investigación en Desarrollo Agroindustrial Sostenible, Universidad de la Costa, CUC,
Calle 58 # 55 - 66. Barranquilla, Colombia

WILEY-VCH
10.1002/cctc.201701223

WILEY-VCH

UPRT shows a remarkable preference for uracil as substrate, and neither thymine nor cytosine can be recognized by any UPRT up to date. However, several bacterial, protozoan and plant UPRTs, such as uracil phosphoribosyltransferase from *Eschericha coli*, *Leishmania donovani* and *Arabidopsis thaliana*, have shown slight activity over different pyrimidine derivatives, such as 4-thiouracil, 6-azauracil or 5-fluorouracil.[5, 23] Unfortunately, an extensive functional characterization of their potential as biocatalysts has not been carried out to date.

Mesophilic enzymes do not usually exhibit high activity and stability under aggressive reaction conditions, such us extreme pH values, high temperatures, or the presence of organic solvents, which are frequently used to circumvent the most habitual problems to scale up bioprocesses from laboratory to industry, e.g. viscosity of the medium and concentration of substrates. The use of enzymes from thermophiles (thermozymes) offers the possibility of using high temperature reactions, resulting in a higher solubilization of substrates, a diminution of medium-viscosity and an increase of substrate diffusion coefficients, leading to higher overall reaction rates.

The present work aims to explore the potential of uracil phosphoribosyltransferase from *Thermus thermophilus* HB8, *Tt*UPRT, as biocatalyst for the synthesis of natural and non-natural NMPs. In this regard, we report here for the first time the cloning of the *uprt* gene from *Thermus thermophilus* HB8, the expression in *Escherichia coli*, purification of the recombinant protein (*Tt*UPRT), and characterization of the enzymatic activity, specificity and oligomeric state of the protein. Furthermore, we also report the complete crystal structure of *Tt*UPRT, which exhibits a canonical PRT fold shared widely with other structurally known UPRTs. Details of active site architecture have also been determined. Our results reveal *Tt*UPRT as a homotetramer, active and stable over a broad temperature range (50-80 °C), pH (5.5-9) and ionic strength (0-500 mM sodium chloride). Specificity studies show that *Tt*UPRT is able to use uracil as base donor (as expected), but surprisingly thymine is also slightly recognized by *Tt*UPRT. More interestingly, *Tt*UPRT is able to recognize several 5 and 6-substituted pyrimidines as substrates, this being the first time that the synthesis of 5-bromouridine-5'-monophosphate, 5-BrUMP, 5-chlorouridine-5'-monophosphate, 5-ClUMP, 5-iodouridine-5'-monophosphate, 5-IUMP, 5-hydroxymethyluridine-5'-monophosphate, 5-OHMeUMP and 6-methyluridine-5'-monophosphate, 6-MeUMP, has been carried out by an UPRT enzyme. All of these features indicate that *Tt*UPRT could be an interesting biocatalyst for the synthesis of different non-natural uridine-5'-monophosphate analogues.

Results and Discussion

Bioinformatics analysis of uracil phosphoribosyltransferase encoding gene of T. thermophilus HB8

The genomic information of *T. thermophilus* HB8 has been analysed and published online (Genbank No. AP008226). Several genes that potentially encode purine and pyrimidine phosphoribosyltransferases were annotated throughout the genome. Among them, two ORFs, *ttha0783* and *ttha1312* (*uprt* gene), which are annotated as putative PyrR bifunctional protein pyrimidine operon regulatory protein/uracil phosphoribosyltransferase and a putative Uracil phosphoribosyltransferase (*Tt*UPRT), were subjected to bioinformatics analyses to identify their physical and chemical properties and possible structures.

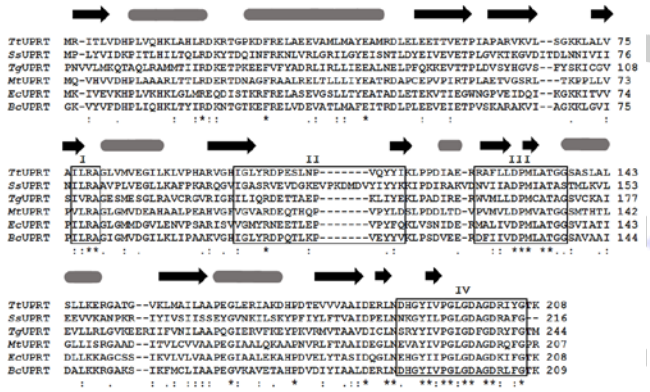

Figure 1. Multiple sequence alignment of uracil phosphoribosyltransferases from *Thermus thermophilus* (*Tt*UPRT), *Sulfolobus sulfotaricus* (*Ss*UPRT), *Toxoplasma gondii* (*Tg*UPRT), *Mycobacterium tuberculosis* (*Mt*UPRT), *Escherichia coli* (*Ec*UPRT) and *Bacillus caldolyticus* (*Bc*UPRT). Amino acid sequences were aligned by CLUSTALΩ. Amino acids for each polypeptide sequence were independently numbered. The secondary structural elements (dark grey cylinder for α helices and black arrows for β strands) for the *Tt*UPRT are indicated above the aligned amino acid sequences. Conserved regions (I-IV) are encircled. *Asterisk* (*) indicates single, fully conserved residues; *colon* (:) indicates conservation of strong groups; and *period* (.) indicates conservation of weak groups.

BLAST analysis of amino acid sequence (http://blast.ncbi.nlm.nih.gov/Blast.cgi) reveals *uprt* encodes a putative uracil phosphoribosyltransferase. The pairwise aminoacid sequence alignment reveals *Tt*UPRT displays high sequence identity with uracil phosphoribosyltransferase from *Bacillus caldolyticus*, *Bc*UPRT, (62 %), *Thermotoga maritima*, *Tm*UPRT (59 %) and *E. coli*, *Ec*UPRT (51 %). The identity percentage with other UPRTs was below 42 %.

Multiple sequence alignment of predicted *Tt*UPRT aminoacid sequence with uracil phosphoribosyltransferases from other thermophilic and mesophilic bacteria and protozoan characterized so far, reveals that 5-phospho-α-D-ribosyl-1-pyrophosphate and uracil binding sites are conserved in *Tt*UPRT sequence (Figure 1). All these characteristics suggest that this gene codes for a putative intracellular uracil phosphoribosyltransferase. *Tt*UPRT was predicted to contain 208 amino acid residues and have a relative molecular mass of 17.66 kDa (Protparam, http://web.expasy.org/protparam). Moreover, multiple sequence alignment of *Tt*UPRT with other homologous UPRTs reveals a high similarity between different UPRTs and clearly suggests that their three-dimensional structures will be very similar, with a conserved core structure encompassing the PRPP/PPi and pyrimidine nucleobase binding sites and sharing similar substrate binding contacts. In this regard, four typical short regions (I–IV) of the UPRTs family, involved in substrate recognition, catalysis, and stability of the protein, can easily be recognized in *Tt*UPRT (Figure 2), a finding which supports a similar active site (Figure 3).[20-22, 24] All described UPRTs contain a conserved PRPP binding domain (region III), thirteen-residue PRPP-binding motif region, which typically comprises four hydrophobic residues followed by two

acidic residues, two hydrophobic residues, and four small residues.[21, 25] In addition, several conserved residues in regions I-II are involved in PRPP binding and stabilization. Near the end C-terminal, bacterial UPRTs display a highly conserved motif (region IV) which is critical in uracil-binding.

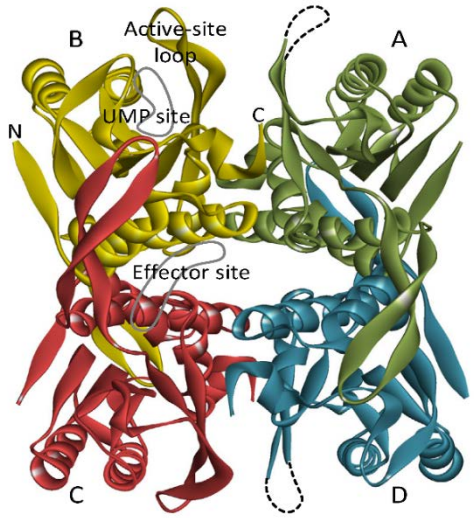

Figure 2. Overall structure of UPRT from *Thermus thermophilus* HB8. A homotetrameric *Tt*UPRT molecule is shown as a ribbon model. Four subunits are distinguished by different coloring and labeling; subunits in open and closed conformations are shown with cool (green and blue) and warm (yellow and red) colors, respectively. The N- and C-termini, the active-site loop, the UMP binding site, and the effector binding site are labeled on subunit B; the binding sites are delineated by gray circles. Invisible active-site loops in subunits A and D are represented as dotted lines. This figure was prepared with Discovery Studio (Accelrys Inc.).

Production and purification of TtUPRT

The *uprt* gene which codes for the uracil phosphoribosyltransferase from *Thermus thermophilus* (*Tt*UPRT), was cloned and overexpressed in *Escherichia coli* BL21(DE3) as described in experimental section. The recombinant N-terminal His6-tagged *Tt*UPRT was purified by two chromatographic steps. SDS-PAGE analysis of purified enzyme shows only one protein band with an apparent molecular mass of 24 kDa (Figure S1). This result agrees with results from analytical ultracentrifugation analysis. Under the conditions assayed, sedimentation velocity experiments revealed *Tt*UPRT as a single specie with an experimental sedimentation coefficient of 5.22 S ($s_{20,w}$ = 5.27) compatible with a tetrameric state (M_w = 98.250 kDa). This value is also compatible with a single-species monomeric model of 24.562 kDa, similar to the molecular mass calculated from the amino acid sequence (24.563 kDa).

Different oligomeric states are described for different bacterial, archaeon and protozoan UPRTs. On the one hand, UPRT from Gram-positive thermophile *Bacillus caldolyticus*, *Bc*UPRT has been described as a dimer,[21] whereas UPRTs from *E. coli*, *Ec*UPRT, and thermoacidophilic archaeon *Sulfolobus solfutaricus*, *Ss*UPRT, were described as a trimer[26] and tetramer[27] respectively. On the other hand, UPRTs from several protozoan parasites, such as *Crithidia luciliae*, *Cl*UPRT,[28] *Giardia lambia*, *Gl*UPRT,[29] and *Toxoplasma gondii*, *Tg*UPRT,[25] were reported as dimers. However, *Tg*UPRT has also been described as monomeric [30] or tetrameric (in presence of GTP which affects the oligomerization state in solution).[31] It seems that the oligomerization state of the PRTs could be essential in catalysis and stabilization of the active conformation as well as in thermal stability of the protein. [20, 32]

Overall structure and architecture of active site

We have determined the crystal structure of *Tt*UPRT (PDB 1v9s) at 2.1 Å resolution (Table 1). The asymmetric unit of *Tt*UPRT crystal contains four subunit chains A, B, C, and D with a canonical PRT fold shared widely with other structurally known UPRTs.[33] These four subunits comprise a homotetramer (Figure 2) which is commonly observed in other reported crystal structures of UPRT from various microorganisms: UPRT from *Thermotoga maritima* (*Tm*UPRT; PDB 1o5o), UPRT from *Escherichia coli* (*Ec*UPRT; PDB 2ehj), UPRT from *Burkholderia pseudomallei* (*Bp*UPRT; PDB 3dmp), UPRT from *Aquifex aeolicus* (*Aa*UPRT; PDB 2e55), UPRT from *Mycobacterium tuberculosis* (*Mt*UPRT; PDB 5e38),[34] UPRT from *Toxoplasma gondii* (*Tg*UPRT; PDB 1bd3/1upu/1jlr/1jls),[25, 31] UPRT from *Sulfolobus solfataricus* (*Ss*UPRT; PDB 1xtt/1xtu/1xtv).[20] In addition, the two subunits A/D or B/C of 1v9s may represent a protomeric homodimer as observed in the crystal structure of UPRT from *Bacillus caldolyticus* (*Bc*UPRT; PDB 1i5e).[21] Although the four subunits in the *Tt*UPRT homotetramer are arranged in the 222 molecular symmetry, two of three pseudo-two fold axes are almost broken, suggesting a structural asymmetry in detail. Of the four subunits, A and D adopt an open conformation in which the active-site pocket is exposed to the solvent due to the disorder of the active-site loop (Arg103−Val111); the root-mean-square deviation (r.m.s.d.) value from the Cα superposition of the open subunits (197 Cα atoms) was 0.303 Å. On the other hand, the subunits B and C adopt a closed conformation in which the active site is covered by the ordered active-site loop and is excluded from the solvent; the r.m.s.d. value for the closed subunits (208 Cα atoms) was 0.234 Å. The Cα superposition from another combination of subunits (197−199 Cα atoms) yielded the higher r.m.s.d. values in the range of 0.417−0.728 Å.

The active-site loop (Arg103−Val111) seems to serve as a flap to open/close the active-site pocket. Interestingly, clear residual electron density compatible with UMP molecule was observed only in the active-site pocket of the closed subunits (B and C), although it was not modeled due to the lack of experimental evidence for identification (Figure 3A). The density may be derived from a co-purified UMP, because we did not add UMP in the crystallization. This putative UMP is recognized by fourteen well-conserved residues in the active-site pocket: the phosphate moiety by Arg103, Ala134, Thr135, Gly136, Gly137, Ser138, the ribose moiety by Arg103, Asp130, Met132, the uracil moiety by Arg103, Met132, Ala134, Gly191, Tyr192, Ile193, Gly198, Asp199, Ala200. Similar co-purified UMP was also reported in *Ss*UPRT (PDB 1xtv).[20] This observation means that only two of four active-site pockets in the tetramer are occupied by UMP, which is reminiscent of the half-of-the-sites reactivity observed in the acyl-CoA thioesterase PaaI from *Thermus thermophilus*,[35] for instance. Another residual electron density, probably for a co-purified effector, was found in the protomeric dimer interface of all four subunits, although we could not estimate the ligand from the shape of the density (Figure 3B).

Table 1. Data collection and refinement statistics.

Data collection	
Space group	$P3_221$
Unit-cell parameters (Å)	a=116.15, c=157.64
Resolution range (Å)	30.0−2.1 (2.18−2.10)
Completeness (%)	99.7 (100.0)
$\langle I/\sigma(I)\rangle$	15.5 (4.4)
[a] R_{merge} (%)	5.1 (29.4)
Refinement	
Resolution range (Å)	30.0−2.1 (2.20−2.10)
[b] R_{cryst} / R_{free} (%)	23.8 (31.2) / 27.3 (35.0)
R.m.s.d. bond lengths (Å)	0.006
R.m.s.d. bond angles (°)	1.30

[a] $R_{merge} = \sum_{hkl} \sum_i |I_i(hkl) - \langle I(hkl)\rangle| / \sum_{hkl} \sum_i I_i(hkl)$, where $I_i(hkl)$ is the ith observation of reflection hkl and $\langle I(hkl)\rangle$ is the weighted average intensity for all observations i of reflection hkl. [b] $R_{cryst} = \sum_{hkl} ||F_{obs}| - |F_{calc}|| / \sum_{hkl} |F_{obs}|$, where $|F_{obs}|$ and $|F_{calc}|$ are the observed and calculated structure-factor amplitudes, respectively. R_{free} was calculated with 5% of the reflections chosen at random and omitted from refinement. Values in parentheses are for the outermost shell.

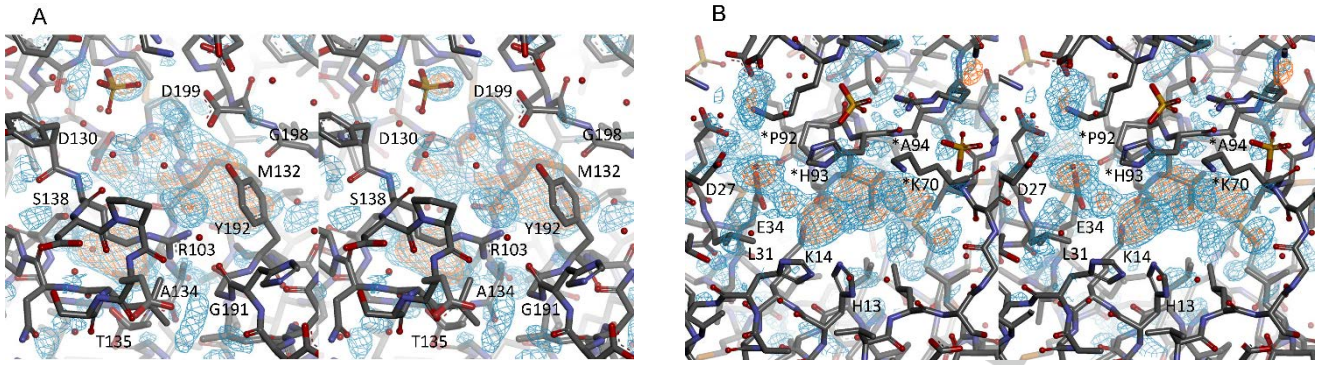

Figure 3. Residual electron densities for putative ligands found in the crystal structure. Stereo representations of crystal structure relevant to the ligand binding in the UMP site of subunit B (*a*) and in the effector site of subunit C (*b*) are shown. Atoms are depicted as stick models with the atom-type coloring. Important residues for ligand recognition are labeled; residues with asterisks denote those on the other subunit. The mF_o−DF_c electron density maps after simulated annealing are overlaid with two different contour levels: 3.0 σ and 4.0 σ for cyan and orange maps, respectively. This figure was prepared with Discovery Studio (Accelrys Inc).

This putative effector site is similar to but distinct from those reported: the CTP site in *Ss*UPRT (PDB 1xtu)[20] and the GTP site in *Tg*UPRT (PDB 1jlr).[31] This putative effector is surrounded by twelve moderately-conserved residues: His13, Lys14, Asp27, Glu30, Leu31, Glu34 from one subunit, and Lys70, Leu71, Val91, Pro92, His93, Ala94 from the other subunit. The invariant arginine residue Arg78, which is reported to be important for an intersubunit communication in *Ss*UPRT (PDB 1xtv),[20] is located in the vicinity of the active-site pocket and adopts the cis main-chain conformation in all four subunits.

In order to elucidate the architecture of the active site, the structural alignment of *Tt*UPRT (PDB 1v9s) was performed with other UPRTs. Three-dimensional superposition with the FATCAT[36] shows mutant Cys128Val *Tg*UPRT as the closest structural homologue (PDB 1bd3; r.m.s.d. of 2.41 Å for 199 Cα atoms and a sequence identity of 35 %), followed in a similar extension by *Tm*UPRT (r.m.s.d. of 3.22 Å for 199 Cα atoms and a sequence identity of 54 %; PDB entry 1o5o) and *Bc*UPRT (r.m.s.d. of 1.35 Å for 199 Cα atoms and a sequence identity of 59 %; PDB 1i5e). According to these results, *Tg*UPRT was chosen as the best candidate for structural alignment (as it is described below).

Substrate specificity

Table 2 summarizes the specific activities of *Tt*UPRT using uracil, thymine and cytosine as acceptors. *Tt*UPRT has a strong preference for uracil, but it also displays activity over thymine. Notably, *Tt*UPRT shows higher specific activities than most other reported UPRTs under similar enzymatic assay conditions. By way of example, for the biosynthesis of UMP, the specific activity showed by *Tt*UPRT (3.7 µmol min^{-1} mg^{-1}) was 1.2, 1.82, 2.4, 6.2 and 26.4 times higher than activity values of UPRTs

from *Giardia intestinalis*, *Gi*UPRT (0.6 µmol min^{-1} mg^{-1});[29] *Toxoplasma gondii*, *Tg*UPRT (2.03 µmol min^{-1} mg^{-1});[30] *Mycobacterium tuberculosis*, *Mt*UPRT (1.7 µmol min^{-1} mg^{-1});[24] *Crithidia luciliae*, *Cl*UPRT (0.6 µmol min^{-1} mg^{-1}; adapted from)[28] and *Sulfolobus shibatae*, *Ss*UPRT, (0.14 µmol min^{-1} mg^{-1}, adapted from),[37] respectively. UPRTase activity of UPRT from *E. coli*, *Ec*UPRT, and *Bacillus caldolyticus*, *Bc*UPRT, is higher than specific activity showed by *Tt*UPRT. However, neither *Ec*UPRT nor *Bc*UPRT exhibit higher thermal stability than *Tt*UPRT, as described below.

Table 2. Reactivity of *Tt*UPRT using different natural pyrimidine bases as substrates

Pyrimidine base[a]	Specific activity (IU/mg_{enz})
Uracil	3.70
Cytosine	n.d.
Thymine	0.80

[a]Reaction conditions were 3 µg of enzyme in 40 µl at 60 °C for 10 min. Substrate concentrations were 10 mM PRPP, 10 mM pyrimidine base, 12 mM $MgCl_2$ in 12 mM TrisHCl buffer, pH 8.0.

Biochemical characterization of TtUPRT

Experimental results reveal that the enzymatic activity of the *Tt*UPRT is strongly dependent on temperature, as expected for proteins from hyperthermophilic organisms. The temperature profile shows that *Tt*UPRT is active (more than 75 %) across a broad temperature range (50-80 °C), with maximum activity at 60 °C (Figure 4A). Interestingly, recombinant *Tt*UPRT also displays high activity (more than 70 %) in a pH range from 5.5 to 9, with maximum activity values at pH 7-8 (Figure 4B). In addition, negligible loss of activity was observed in presence of 500 mM of sodium chloride, and a slight activity decrease was observed when sodium chloride concentration was increased (70 % activity remained at 1 M sodium chloride) (Figure 4C).

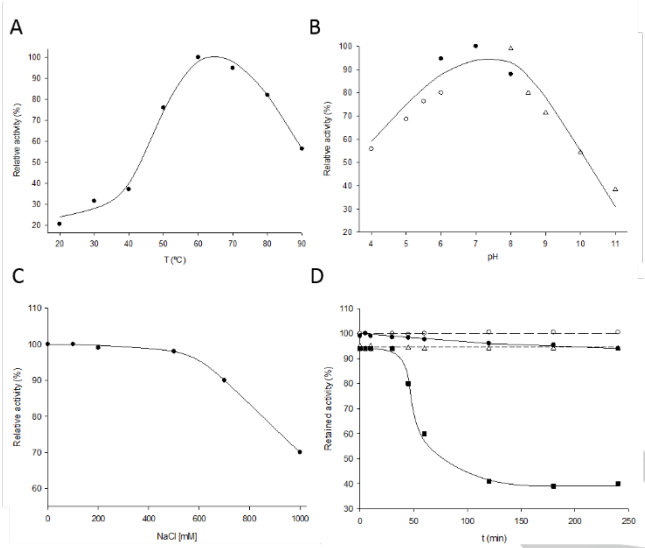

Figure 4. Temperature and pH dependence on *Tt*UPRT activity and stability. **A)** Effect of temperature on *Tt*UPRT activity (●). **B)** Effect of pH on *Tt*UPRT activity, (○) sodium acetate 50 mM (pH 4-6), (●) sodium phosphate 50 mM (pH 6-8), (Δ) sodium borate 50 mM (pH 8-10). **C)** Effect of ionic strenght on *Tt*UPRT activity **D)** (●). Thermal inactivation of *Tt*UPRT in 20 mM Tris-HCl buffer, pH 8.0 at different temperatures 50 °C (Δ), 60 °C (○), 70 °C (●) and 80 °C (■).

Steady-state kinetics

Steady-state kinetic studies were carried out at variable concentrations of uracil or PRPP, in order to determine K_M, k_{cat} and k_{cat}/K_M values. The results are summarized in Table 3. *Tt*UPRT shows lower K_M values for uracil than for PRPP. These results agree with kinetic data described for other UPRTs, [21, 22, 24, 27, 29]. In this sense, it is reasonable to think that similar to other UPRTs, catalysis could follow a sequential mechanism, in which PRPP binding is followed by uracil, and PPi product is released first, followed by UMP

Table 3. Steady-state kinetic parameters for UMP formation reaction catalyzed by *Tt*UPRT.

Variable uracil[a]			Variable PRPP[b]		
K_M (mM)	k_{cat} (s^{-1})	k_{cat}/K_M (s^{-1} mM^{-1})	K_M (mM)	k_{cat} (s^{-1})	k_{cat}/K_M (s^{-1} mM^{-1})
0.19±0.03	28.87±0.5	151.94	3.33±0.7	44.32±1.3	13.30

[a] Concentration range 0.12-17 mM at a fixed PRPP concentration of 10 mM.
[b] Concentration range 0.25-32 mM at a fixed Uracil concentration of 10 mM.

Biocatalyst stability

Some enzymes, especially in partially purified preparations, may be remarkably unstable, losing a significant amount of activity over the period of incubation. In this sense, it is necessary to determine if the enzyme is active and stable under operational conditions.The stability of a biocatalyst is defined as the time during which it retains 50 % of its initial activity and is affected by environmental conditions such as pH and temperature.

Storage of *Tt*UPRT at 4 °C was analysed to ensure enzyme stability, and *Tt*UPRT retained its activity for more than 130 days (85 % relative activity) (data not shown). Unfortunately, activity decreased considerably (25 % of retained activity) when stored at -20 °C or -80 °C.

In addition, the effect of temperature on enzyme stability was evaluated by incubating *Tt*UPRT in 20 mM Tris-HCl, pH 8.0 at different temperatures (50-80 °C) during 2 hours (Figure 4D). Experimental data shows that *Tt*UPRT is stable in a temperature range from 50 to 70 °C, whereas unfortunately *Tt*UPRT undergoes a significant loss of activity when stored at 80 °C for incubation periods of more than 45 min, probably due to protein suffering irreversible denaturation. These results agree with thermostability of UPRT from extreme thermoacidophilic archaebacterium *Sulfolobus shibatae*, which displays tolerated incubation at 80 °C for at least one hour without detectable loss of activity. In addition, both enzymes, *Tt*UPRT and *Ss*UPRT, exhibit higher stability than other described UPRTs, such as UPRT from Gram-positive thermophile *Bacillus caldolyticus*, *Bc*UPRT (60 % of retained activity at 70 °C),[38] and mesohophilic UPRTs from *B. subtillis*, *Bs*UPRT (40 % of retained activity at 52 °C),[38] and *Toxoplasma gondii*, *Tg*UPRT(completely inactivated by heating for 5 min at 65 °C).[30]

Enzymatic production of natural and non-natural NMPs

In order to assess the potential of *Tt*UPRT as biocatalyst, it was performed the enzymatic production of different NMP analogues using different pyrimidine bases as substrates (Table 4). Interestingly, *Tt*UPRT shows activity towards unusual substrates,

such us thymine, 5-halogenated uracil derivatives, 5-hidroxymethyluracil and 6-methyluracil (Scheme 1). Among them, *Tt*UPRT employed these non-natural bases as acceptors in the following order of preference: Thymine > 5-FUra ≈ 5-ClUra > 5-BrUra > 5-IUra >> 5-OHMeUra > 6-MetUra. Despite the fact that several bacterial and protozoan UPRTs, such as uracil phosphoribosyltransferase from *Eschericha coli* or *Leishmania donovani*, are able to act on different pyrimidine derivatives, such as 4-thiouracil, 6-azauracil or 5-fluorouracil,[5] none of the reported UPRTs displayed activity over thymine and the following non-natural uracil derivatives, 5-chlorouracil, 5-bromouracil, 5-iodouracil, 5-hydroxymethyluracil and 6-methyluracil). On the contrary, other uracil derivatives, such as 5-ethyluracil, 6-methyl-2-thiouracil, 6-propyl-2-thiouracil, 2-methoxy-5-fluorouracil and (E)-5-(2-bromovinyl) uracil, were not recognized as substrates. Furthermore, neither cytosine (cytosine, 5-methylcytosine, 5-fluorocytosine and 5-azacytosine) nor thymine derivatives (trifluorothymine) could be recognized by *Tt*UPRT.

Table 4. Enzymatic production of natural and non-natural NMPs

Pyrimidine base[a]	Conversion (%)
Uracil	50
5-fluorouracil	18
5-chlorouracil	17
5-bromouracil	12
5-iodouracil	12
5-ethyluracil	n.d.
5-hydroxymethyluracil	8
6-methyluracil	5
6-methyl-2-thiouracil	n.d.
6-propyl-2-thiouracil	n.d.
(E)-5-(2-bromovinyl)uracil	n.d.
Cytosine	n.d.
5-methylcytosine	n.d.
5-fluorocytosine	n.d.
5-azacytosine	n.d.
Thymine	20
Trifluorothymine	n.d.
5-fluoro-2-methoxy-4(1H)pirimidinone	n.d.

[a]Reaction conditions were 3 µg of enzyme in 40 µl at 60 °C for 15-45 min. Substrate concentrations were 1 mM PRPP, 1 mM modified pyrimidine base, 1.2 mM $MgCl_2$ in 12 mM TrisHCl buffer, pH 8.0.
nd: not detected

These results do not totally agree with previous reports which state that UPRT displays a strict specificity over uracil and does not act on cytosine or thymine.[24-25, 27, 38] Itzsch and Tankerslay[39] performed a structure-activity study, in which 100 compounds were evaluated as ligands of uracil phosphoribosyltransferase from *Toxoplasma gondii* (*Tg*UPRT) by examining their ability to inhibit UMP synthesis. Their study reveals that methylene group in position 5 is strongly preferred. Consequently, large exocyclic substituents at this position decrease (fluoro) or abolish (bromo) base binding; substituents larger than hydrogen also abolish binding to UPRT. This supposed consequence of larger volumes at position 5 causes a steric hindrance in the active site. Unfortunately, neither of the aforementioned studies used these substrates in the synthesis of corresponding NMPs, so we could not know if *Tg*UPRT really can act on them.

In 1998, Schumacher et al.[25] reported the structures of UPRT from *T. gondii* both in Apo and bonded with uracil and 5-fluorouracil (PDBs 1bd3, 1bd4 and 1fpU respectively). This work allowed them to get a better understanding about the substrate specificity studies previously described by Itzsch and Tankerslay.[39] The structural alignment of 5-fluorouracil complexed *Tg*UPRT with uracil complex reveals minor adjustments in the active-site residues, especially in the base binding site (Figure 5A). As described for uracil, the molecule stacks between Met166 and Thr228 and forms 4 hydrogen bonds with active-site residues, one water mediated. The main difference between the binding of uracil and 5-fluorouracil is a small rotation in the latter in order to avoid steric clash with Ala168 Cβ (the distance between 5-fluoro and Ala168 Cβ is 3.1 Å). Consequently, the failure binding of 5-iodo-, 5-bromo or 5-chloro is related to the longer carbon-halogen bond and their larger van der Waals radius which results in steric hindrance with Ala168 Cβ.

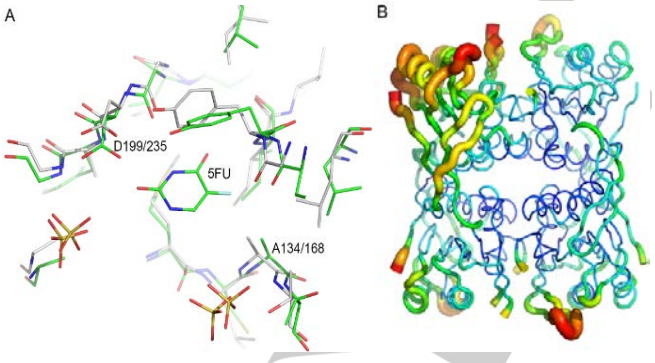

Figure 5. A) Superposition of base binding site of *Toxoplasma gondii* UPRT in complex with 5-fluorouracil (green) and *Thermus thermophilus* UPRT (white). The reduction or absence of enzymatic activity over substituents at position 5 is attributed to steric hindrance of position 5 with Ala168 Cβ in *Tg*UPRT. However, *Tt*UPRT is able to bind and catalyze these modified uracil nucleosides. **B)** Tube mode in B-factor gradient of the *Tt*UPRT. The most mobile parts of the protein are shown in yellow and red. The turn which lies residue Tyr192 involved in π-stacking with uracil molecule is the one with the highest B factors.

However, a different scenario is observed for *Tt*UPRT, which not only recognizes uracil and 5-fluorouracil but is able to recognize thymine, 5-chloro-, 5-bromo-, 5-iodouracil and 5-hydroxymethyluracil as substrates. Comparison by superposition with *Tg*UPRT shows an r.m.s.d. of 3.0 and 1.9 Å for tetramer and monomer, respectively. Comparing base binding site (BBS) of *Tt*UPRT reveals a conserved site (Figure 5A), although some differences are observed in the vicinity of BBS residues. These differences involve a substitution to glycine, which increases the mobility of these regions (A170G136 and Y227G191, *Tg*UPRT:*Tt*UPRT). Another substitution observed is F236A200. Indeed, the region of Y192 is a β-turn and has higher B-factors indicating an increased flexibility of this region (Figure 5B). As result of these differences, we could assume an increase of the active-site size, and therefore *Tt*UPRT, as demonstrated by enzymatic assays, is able to bind and catalyze 5-uracil substituents. Nevertheless, substituents larger than hydrogen at position 6 causes a steric hindrance in the active site, producing lower or not detected activities of *Tt*UPRT.

Conclusions

Herein we describe for the first time the full structural and biochemical characterization of uracil phosphoribosyltransferase from *Thermus thermophilus* HB8, *Tt*UPRT, that present significant catalytic activity in a broad range of pH (from 5.5 to 9) and temperature interval (from 50 to 80 °C). The thermophilic origin of *Tt*UPRT shows several associated advantages, such as an easy purification method and thermostability at high temperatures (50 to 80 °C). Excitingly, the ability of *Tt*UPRT to accept position 5-substituted pyrimidines is especially interesting, since these are positions commonly substituted in nucleotide analogues used for the treatment of human diseases, which makes this enzyme attractive for the industrial synthesis of nucleoside derivatives.

Experimental Details

Materials

Cell culture medium reagents were from Difco (St. Louis, MO). Trimethyl ammonium acetate buffer and 5-phospho-α-D-ribosyl-1-pyrophosphate were purchased from Sigma-Aldrich (USA). All other reagents and organic solvents were purchased from Scharlab (Barcelona, Spain) and Symta (Madrid, Spain). All natural and non-natural purine bases used were provided by Carbosynth Ltd. (Compton, United Kingdom).

Enzyme Cloning, Expression and Purification

Two different protocols were used in this study, one for biochemical characterization and the other for crystallization and structure determination.

The encoding *ttha1312* gene (*uprt* gene), which codifies uracil phosphoribosyltransferase from *Thermus thermophilus* HB8 (NCBI Reference Sequence: YP_144578.1), was ordered and purchased from Genscript (Piscataway, USA). The coding sequence appeared as an *Nde*I-*Bam*HI fragment subcloned into the expression vector pET28b (+). The resultant recombinant vector pET28b*Tt*UPRT provided an N-terminal His6-tagged fusion with a thrombin cleavage site between the tag and the enzyme. *Tt*UPRT was expressed in *E. coli* BL21(DE3) grown in Luria-Bertani medium at 37 °C with kanamycin 50 μg/mL. Protein overexpression was induced by adding 0.5 mM isopropyl-β-D-1-thiogalactopyranoside and the cells further grown for 10 hours. These were harvested via centrifugation at 3500 x *g*. The resulting pellet was resuspended in 20 mM Tris-HCl, pH 8.0, containing 100 mM sodium chloride. Crude extracts were prepared by ultrasonic cell treatment using a digital sonifier. The lysate was centrifuged at 17500 x *g* for 20 min at 4 °C, and then heated at 70 °C for 20 min. Insoluble material was removed by centrifugation 17500 x *g* for 20 min at 4 °C, and the supernatant was filtered through a 0.22 μm filter (Millipore). Cleared lysate was loaded onto a 5-mL HisTrap FF column (GE Healthcare) pre-equilibrated in a binding buffer (20 mM Tris-HCl buffer, pH 8.0, with 100 mM sodium chloride and 10 mM imidazole) and the column was washed. Bound proteins were eluted using a linear gradient of imidazole (from 10 to 500 mM). Fractions containing *Tt*UPRT were identified by SDS-PAGE, pooled, concentrated and loaded onto a HiLoad 16/60 Superdex 200 prep grade column (GE Healthcare) pre-equilibrated in 20 mM Tris-HCl, pH 8.0. Fractions with the protein of interest identified by SDS-PAGE were pooled and the protein was concentrated and stored at 4 °C until its use. Electrophoresis was carried out on 15 % polyacrylamide slab gel with 25 mM Tris-HCl buffer, pH 8.6, 0.1 % SDS. Protein concentration was determined spectrophotometrically by UV absorption at 280 nm using a ε_{280}= 8940 M^{-1} cm^{-1}.[40]

*Tt*UPRT expression and purification for crystallization and structure determination were carried out according to a different protocol. For structural determination, *Tt*UPRT was expressed as a selenomethionine (SeMet)-substituted protein. The plasmid encoding *Tt*UPRT protein was digested with *Nde*I and *Bam*HI and the fragment was inserted into the expression vector pET-11a linearized with *Nde*I and *Bam*HI. The recombinant plasmid was transformed into *Escherichia coli* B834(DE3)plysS cells and grown at 37 °C in M9 medium until absorbance of the medium at 600 nm reached 0.4. At this point, 100 mg of L-lysine, 100 mg of L-phenylalanine, 100 mg of L-threonine, 50 mg of L-isoleucine, 50 mg of L-leucine, and 60 mg of SeMet were added to 1 L of culture and the cells were grown at 37 °C for a further 1 h, before inducing the expression with 1 mM IPTG overnight at 25 °C. The cells were harvested by centrifugation. The cell pellet was suspended in 20 mM Tris-HCl, pH 8.0, containing 0.5 M sodium chloride and 5 mM 2-mercaptoethanol, and homogenized by ultrasonication. The supernatant of the crude extract was heated at 70 °C for 12 min and the cell debris and denatured proteins were removed by centrifugation. The heat-treated extract was desalted by HiPrep 26/10 desalting column and applied onto a Super Q Toyopearl 650M column equilibrated with 20 mM Tris-HCl, pH 8.0. Proteins were eluted with a linear gradient of 0−0.3 M sodium chloride. The fractions containing proteins were then dialyzed against 20 mM Tris-HCl, pH 8.0, and subjected to Resource Q column (Amersham Biosciences) equilibrated with 20 mM Tris-HCl, pH 8.0. Proteins were again eluted with a linear gradient of 0−0.3 M sodium chloride. The fractions containing proteins were desalted with HiPrep 26/10 desalting column with 10 mM sodium phosphate, pH 7.0, and applied onto a Bio-Scale CHT20-I column (Bio-Rad) equilibrated with 10 mM sodium phosphate, pH 7.0. Proteins were again eluted with a linear gradient of 10−100 mM sodium phosphate. The fractions containing proteins were concentrated by ultrafiltration (Vivaspin) and loaded onto a HiLoad 16/60 Superdex 75 pg column (Amersham Biosciences) equilibrated with 20 mM Tris-HCl, pH 8.0, containing 0.2 M sodium chloride. The homogeneity and identity of the purified sample were ascertained by SDS-PAGE and N-terminal sequence analysis. Finally, the purified *Tt*UPRT with SeMet substitution was concentrated to 12.0 mg/mL by ultrafiltration.

Analytical ultracentrifugation analysis

Sedimentation velocity experiments for *Tt*UPRT were carried out in 20 mM Tris-HCl, pH 8.0 at 20 °C and 50,000 × *g* in an Optima XL-I analytical ultracentrifuge (Beckman-Coulter Inc.), equipped with UV-VIS absorbance and Raleigh interference detection systems, using an An-60Ti rotor and standard (12 mm optical path) double-sector centre pieces of Epon-charcoal. Sedimentation profiles were recorded at 292 nm. Sedimentation coefficient distributions were calculated by least-squares boundary modelling of sedimentation velocity using the continuous distribution *c(s)* Lamm equation model as implemented by SEDFIT 14.7g.
Baseline offsets were measured afterwards at 200,000 × *g*. The apparent sedimentation coefficient of distribution, *c(s)*, and sedimentation coefficient, *s*, were calculated from the sedimentation velocity data using the SEDFIT program.[41] The

experimental sedimentation coefficients were corrected to standard conditions (water, 20 °C, and infinite dilution) using SEDNTERP software [42] to obtain the corresponding standard s values ($s_{20,w}$).

Crystallization, data collection and structure determination.

Crystals of *Tt*UPRT were obtained with the oil-microbatch method using NUNC HLA plates (Nalge Nunc International). Each crystallization drop was prepared by mixing 1.0 µL of the precipitant solution (0.2 M ammonium sulfate, 0.1 M sodium citrate, 0.1 M dioxane, pH 5.5) and 1.0 µL of the protein solution (SeMet-substituted *Tt*UPRT at 12.0 mg/mL). Then the crystallization drop was overlaid by 1:1 mixture of silicon/paraffin oils, allowing a slow evaporation of water in the drop. The crystals grew to full size in 3−4 days. For the collection of diffraction data, the crystals were soaked in the precipitant solution containing 20 % (v/v) glycerol as a cryoprotectant and flash-frozen with liquid nitrogen. Complete data sets were collected using a RIGAKU CCD detector at the synchrotron beam line BL26B1 at SPring-8, Japan. The data were processed and scaled using the HKL 2000 program suite.[43] Data collection statistics are given in Table 1.
The crystal structure of *Tt*UPRT was determined by the multiple anomalous dispersion method [44] using the anomalous dispersion effect from selenium atoms in the SeMet-sustituted protein. The Se-atom coordinates and initial electron density map were obtained with the SOLVE/RESOLVE program.[45] The protein model was built and improved manually with the program QUANTA2000 (Accelrys Inc.) and refined with the CNS program.[46] The stereo-chemical quality of the model was checked with the PROCHECK program.[47] The refinement statistics are summarized in Table 1. The final atomic coordinates were deposited in the RCSB Protein Data Bank with the accession code 1v9s. Superposition analysis was performed using the program LSQKAB[48] in the CCP4 program suite.[49]

Enzyme activity assay

The standard activity assay was performed by incubating 10 µL of free extract or 3 µg of pure His-tag enzyme with 10 mM PRPP, 10 mM uracil (or thymine or cytosine), 12 mM $MgCl_2$ in 12 mM TrisHCl buffer pH 8.0 in a final volume of 40 µL. The reaction mixture was incubated at 60 °C for 10 min (300 rpm). Enzyme was inactivated by adding 40 µL of cold methanol in ice-bath and heating for 5 min at 100 °C. After centrifugation at 9000 × *g* for 5 min, samples were half-diluted with water and the NMP production was analysed by HPLC to quantitatively measure the reaction products as described below in the analytical methods. All determinations were carried out in triplicate and the maximum error was below 5 %. In such conditions, one international activity unit (IU) was defined as the amount of enzyme producing 1 µmol/min of UMP under the assay conditions.

Enzymatic production of natural and non-natural nucleosides-5´-monophosphate from pyrimidine bases

Enzymatic production of natural and non-natural NMPs was carried out by incubating 3 µg of pure His-tag enzyme with 1 mM PRPP, 1 mM natural or non-natural pyrimidine base and 1.2 mM MgCl2 in 12 mM Tris-HCl buffer pH 8.0. The reaction mixtures were incubated at 60 °C and 300 rpm orbital shaking at different reaction times (15-45 min). Subsequently, the reaction mixture was processed as described above and the NMP production was analysed by HPLC.

Kinetic parameters and initial velocity pattern

The steady-state kinetic parameters, K_M, k_{cat} and V_{max}, were determined under standard assay conditions at varying concentrations of one substrate (0.12-17 mM for Uracil, 0.25-32 mM for PRPP), while the concentration of the other substrate was fixed at constant saturating level (10 mM). Apparent K_M, k_{cat} and k_{cat}/K_M values were determined by non-linear regression assuming Michaelis–Menten kinetics. Calculations were carried out using the Origin program from Origin Lab Corporation.

Influence of pH, temperature and ionic strength on enzyme activity

The optimum pH of the His-tag enzyme was initially determined according to the standard activity assay described above, using sodium citrate (pH 4-6), sodium phosphate (pH 6-8) and sodium borate (pH 8-10) as reaction buffers (50 mM). The optimum temperature was determined using standard assay in 20 - 90 °C temperature range. A similar approach was used to characterize the effect of ionic strength on enzyme activity. *Tt*UPRT activity was measured at different concentrations of sodium chloride, ranging from 0 to 1 M.

Thermal and pH stability of TtUPRT

His-tag *Tt*UPRT was stored at 4 °C in 20 mM Tris-HCl buffer, pH 8.0 for 100 days. Samples were taken periodically, and enzymatic activity was evaluated. Storage stability was defined as the relative activity between the first reaction and successive reactions. Moreover, thermal stability of *Tt*UPRT was performed by incubating 3 µg of pure His-tag enzyme in 20 mM Tris-HCl buffer, pH 8.0 at different temperatures (50-90 °C) and different storage times (15-120 min). After cooling, the samples were assayed for UPRTase activity under standard conditions.

Analytical methods

The production of NMPs was quantitatively measured with an ACE EXCEL 5 µm CN-ES 250 × 4.6 mm equilibrated with 100 % trimethyl ammonium acetate at a flow rate of 0.8 mL/min. Retention times for the reference natural compounds (hereafter abbreviated according to the recommendations of the IUPAC-IUB Commission on Biochemical Nomenclature) were as follows: uracil (Ura), 4.6 min; uridine-5'- monophosphate (UMP), 3.5 min; cytosine (Cyt), 4.1 min; cytidine-5'-monophosphate (CMP), 3.1 min; thymine (Thy), 7.2 min; thymidine-5'-monophosphate (TMP), 4.4 min. Retention times for the reference non-natural bases (hereafter abbreviated according to the recommendations of the IUPAC-IUB Commission on Biochemical Nomenclature) were as follows: 5-fluorouracil (5-FUra), 5.4 min; 5-fluorouridine-5'- monophosphate (5-FUMP), 3.6 min; 5-chlorouracil (5-ClUra), 8.5 min; 5-chlorouridine-5'-monophosphate (5-ClUMP), 3.9 min; 5-bromouracil (5-BrUra), 10.5 min; 5-bromouridine-5'- monophosphate (5-BrUMP), 4.3 min; 5-iodouracil (5-IUra), 15.0 min; 5-iodouridine-5'-monophosphate (5-IUMP), 5.3 min; 5-hydroxymethyluracil (5-OHMeUra), 4.4 min; 5-hydroxymethyluridine-5'-monophosphate (5-OHMeUMP), 3.6 min; 6-methyluracil (6-MeUra): 6.3 min; 6-

methyluridine monophosphate (6-MeUMP): 3.7 min; 5-azacytosine (5-AzaCyt), 3.7 min; 5-fluorocytosine (5-FCyt): 4.0 min; 5-ethyluracil (5-EtUra), 12 min; 6-methyl-2-thiouracil (6-MetThioUra), 13.5 min; 6-propyl-2-thiouracil (6-PropThioUra), 19.0 min; 5-(2-bromovinyl)uracil, (5-BrVinUra), 26 min; 5-fluoro-2-methoxy-4(1H) pyrimidinone, (5-FMP), 5 min; 6-azauracil (6-azaUra), 4.1 min; Trifluorothymine (TFT), 19.0 min. Results were normalized based on the nucleobase mass balance.

Acknowledgments

We thank Peter Bonney for their continued support and enthusiasm for the project. This work was supported by grant SAN151610 from the Santander Foundation. Grant 2016/UEM8 from Universidad Europea de Madrid is also acknowledged.

Keywords: biocatalysis • uracil phosphoribosyltransferase • thermophiles • nucleoside-5'-monophosphates • crystallization

[1] E. De Clercq, *Antiviral Res.* **2005**, *67*, 56-75.
[2] C.M. Galmarini, J.R. Mackey, C. Dumontet. *Lancet Oncol*. **2002**, *3*, 415-424.
[3] W.B. Parker, *Chem. Rev*. **2009**, *109*, 2880-2893.
[4] B. Roy, A. Depaix, C. Périgaud, S. Peyrottes, *Chem. Rev.* **2016**, *116*, 7854-7897.
[5] L.E. Iglesias, E.S. Lewkowicz, R. Medici, P. Bianchi, A.M. Iribarren, *Biotechnol. Adv*. **2015**, *33*, 412-434.
[6] M., Yoshikawa, T. Kato, T. Takenishi, *Bull. Chem. Soc. Jpn.* **1969**, *42*, 3505–3508.
[7] A. Fresco-Taboada, I. de la Mata, M. Arroyo, J. Fernández-Lucas, *Appl Microbiol Biotechnol*, **2013**, *97*, 3773-3785.
[8] J. Fernández-Lucas, *Appl. Microbiol. Biotechnol.* **2015**, *99*, 4615-4627.
[9] Y. Li, Q. Ding, L. Ou, Y. Qian, J. Zhang, *Biotechnol. Bioprocess Eng.* **2015**, *20*, 37-43.
[10 Zou, Q. Ding, L. Ou, B. Yan, *Appl. Microbiol. Biotechnol*. **2013**, *97*, 9389-9395.
[11] R.A. Scism, D.F. Stec, B.O. Bachmann, *Org. Lett*. **2007**, *9*, 4179-4182.
[12] R.A. Scism, B.O. Bachmann, *ChemBioChem* **2010**, *11*, 67-70.
[13] H. Mori, A. Iida, S. Teshiba, T. Fujio, *J. Bacteriol*. **1995**, *177*, 4921-4926.
[14] H. Mori, A. Iida, T. Fujio, S. Teshiba, *Appl. Microbiol. Biotechnol*. **1997**, *48*, 693-698.
[15] I. Serra, S. Conti, J. Piškur, A.R. Clausen, B. Munch-Petersen, M. Terreni, D. Ubiali, *Adv. Synth. Catal*. **2014**, *356*, 563-570.
[16] Z.Q. Liu, L. Zhang, L.H. Sun, X.J. Li, N.W. Wan, Y.G. Zheng, *Food Chem*. **2012**, *134*, 948-956.
[17] Y. Mihara, T. Utagawa, H. Yamada, Y. Asano, *Appl. Environ. Microbiol.* **2000**, *66*, 2811-2816.
[18] H. Zou, G. Cai, W. Cai, H. Li, Y. Gu, Y. Park, F. Meng, *Tsinghua Sci. Technol*. **2008**, *13*, 480-484.
[19] J. Del Arco, M. Martinez, M. Donday, V. Clemente-Suarez, J. Fernández-Lucas, *Biocatal. Biotransfor*. **2017**, 1-8.
[20] S. Arent, P. Harris, K.F. Jensen, S. Larsen, *Biochemistry* **2005**, *44*, 883-892.
[21] A. Kadziola, J. Neuhard, S. Larsen, *Acta Crystallogr. D Biol. Crystallogr*. **2002**, *58*, 936-945.
[22] C. Lundegaard, K.F. Jensen, *Biochemistry* **1999**, *38*, 3327-3334.
[23] S. Narayanan, P. Sanpui, L. Sahoo, S.S. Ghosh, *Int. J. Biol. Macromolec*. **2016**, *91*, 310-316
[24] A.D. Villela, R.G. Ducati, L.A. Rosado, C.J. Bloch, M.V. Prates, D.C. Gonçalves, C.H.I. Ramos, L.A. Basso, D.S. Santos, *PLOS ONE* **2013**, *8*, 1-14.
[25] M.A. Schumacher, D. Carter, D.M. Scott, D.S. Roos, B. Ullman, R.G. Brennan, *EMBO J.* **1998**, *17*, 3219-3232.
[26] S. Christofferse, A. Kadziola, E. Johansson, M. Rasmussen, M. Willemoës, K.F. Jensen, *J. Mol. Biol.* **2009**, *393*, 464-477.
[27] U.B. Rasmussen, B. Mygind, N. Per, *BBA-Gen. Subjects* **1986**, *881*, 268-275.
[28] T. Asai, C.S. Lee, A. Chandler, W.J. O'Sullivan, *Comp. Biochem. Physiol. B-Biochem. Mol.* **1990**, *95*, 159-163.
[29] Y.P. Dai, C.S. Lee, W.J. O'Sullivan, *Int. J. Parasitol*. **1995**, *25*, 207–214.
[30] D. Carter, R.G. Donald, D. Roos, B. Ullman, *Mol. Biochem. Parasitol*. **1997**, *87*, 137-144.
[31] M.A. Schumacher, C.J. Bashor, M.H. Song, K. Otsu, S. Zhu, R. Parry, R.J., B. Ullman, R.G. Brennan, *PNAS*, **2002**, *99*, 78-83.
[32] D. de Souza Dantas, C.R. dos Santos, G.A.G. Pereira, F.J. Medrano, *BBA. Proteins Proteom*. **2008**, *1784*, 953-960.
[33] S.C. Sinha, J.L. Smith, *Curr. Opin. Struct. Biol.* **2001**, *11*, 733−739.
[34] P. Ghode, C. Jobichen, S. Ramachandran, P. Bifani, J. Sivaraman, *Biochem. Biophys. Res. Commun*. **2015**, *467*, 577−582.
[35] N. Kunishima, Y. Asada, M. Sugahara, J. Ishijima, Y. Nodake, M. Sugahara, M. Miyano, S. Kuramitsu, S. Yokoyama, M. Sugahara, *J. Mol. Biol*. **2005**, *352*, 212−228
[36] Z. Li, Y. Ye, A. Godzik, *Nucleic Acids Res*. **2006**, *34*, D277-D280.
[37] L. Linde, K.F. Jensen, BBA-Protein. Struct. M. **1996**, *1296*, 16-22.
[38] H. K. Jensen, N. Mikkelsen, J. Neuhard. *Protein Expr. Purif.* **1997**, *10*, 356-364.
[39] M.H. Iltzsch, K.O. Tankersley, *Biochem. Pharmacol.* **1994**, *48*, 781-791.
[40] S.C. Gill, P.H. Von Hippel, *Anal. Biochem*. **1989**, *182*, 319-326.
[41] P.H. Brown, P. Schuck, *Biophys. J*. **2006**, *90*, 398 4651-4661.
[42] Holde K.E, *Physical Biochemistry* **1985**, 2nd Ed., Prentice-Hall, Englewood Cliffs, 440 N.
[43] Z. Otwinowski, W. Minor, *Meth. Enzymol.* **1997**, *276*, 307–326.
[44] W.A. Hendrickson, J.R. Horton, D.M. LeMaster. *EMBO J.* **1990**, *9*, 1665−1672.
[45] T.C. Terwilliger, J. Berendzen, *Acta Crystallogr. D Biol. Crystallogr*. **1999**, *55*, 849−861.
[46] A.T. Brünger, P.D. Adams, G.M. Clore, W.L. DeLano, P. Gross, R.W. Grosse-Kunstleve, J.S. Jiang, J. Kuszewski, M. Nilges, N.S. Pannu, R.J Read, L.M. Rice, T. Simonson, G.L. Warren, *Acta Crystallogr. D Biol. Crystallogr*. **1998**, *54*, 905–921.
[47] R.A. Laskowski, M.W. MacArthur, D.S. Moss, J.M. Thornton, *J. Appl. Crystallogr.* **1993**, *26*, 283−291.
[48] W.A. Kabsch, *Acta Crystallogr*. A **1976**, *32*, 922−923.
[49] M.D. Winn, C.C. Ballard, K.D. Cowtan, E.J. Dodson, P. Emsley, P.R. Evans, R.M. Keegan, E.B. Krissinel, A.G. Leslie, A. McCoy, S.J. McNicholas, G.N. Murshudov, N.S. Pannu, E.A. Potterton, H.R. Powell, R.J. Read, A. Vagin, K.S. Wilson, *Acta Crystallogr. D Biol. Crystallogr*. **2011**, *67*, 235−242.

10.1002/cctc.201701223

WILEY-VCH

FULL PAPER

Text for Table of Contents

The enzymatic production of several modified nucleoside-5'-monophosphates has been performed by uracil phosphoribosyltransferase from *Thermus themophilus*,*Tt*UPRT. In addition, the functional and structural characterization of *Tt*UPRT has been reported for first time.

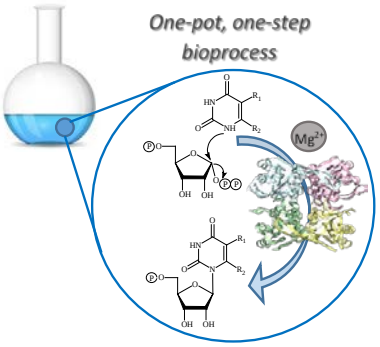

Authors: *Jon del Arco,[a] Javier Acosta,[a] Humberto M. Pereira,[b] Almudena Perona,[a] Neratur K. Lokanath,[c] Naoki Kunishima, * [d] Jesús Fernández-Lucas * [a, e].*

Page No. – Page No.

Title: *Enzymatic production of non-natural nucleoside-5'-monophosphates by a novel thermostable uracil phosphoribosyltransferase*